4.3 Booster Synchrotron. Sub-systems.

The larger diameter booster synchrotron option significantly simplifies the design features of the main sub-systems of the machine; the magnets, vacuum and power supply systems. An important part of the booster subsystem is the beam parameters for the diagnostic and control system to provide effective injection and extraction, and to maintain reproducible electron beam in all three modes of storage ring operation: single and multi-bunch modes, top-up injection into the storage ring.
Since the booster synchrotron will be mounted on the inner wall of the main storage ring tunnel, a compact design for the magnets and the vacuum chamber is of significant importance.

4.3.1 Magnets

The magnetic lattice of the booster synchrotron consists of 48 separated function dipole magnets, 64 quadrupole magnets, 56 sextupole magnets and 32 corrector magnets. The regular lattice of the booster synchrotron with the cross section of the vacuum chamber is shown in Fig. 4.3.1. The regular lattice is the usual FODO cell with two dipole magnets. Sixteen cells are arranged with a missing dipole to provide dispersion-free straight sections for beam injection and extraction, as well as for RF cavity installation.

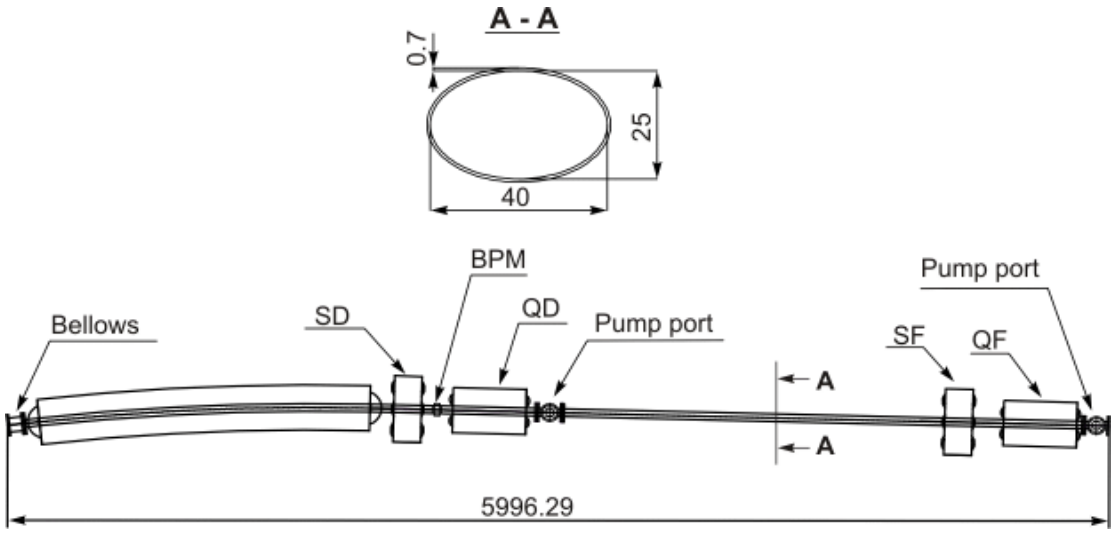

Fig. 4.3.1 Magnetic cell of the booster synchrotron with missing dipole.

Dipole Magnet.
Our choice for the booster bending magnet is an H-type dipole. The parameters defining design are listed in the Table 4.3.1. With the distance between booster and storage ring minimally being 2.8 m, stray fields from booster magnets may influence the storage ring beam. H-type shape closed yoke magnets are a good choice to minimize those stray fields. To allow access to the pole area and to mount the coils, the magnet yoke is divided at the horizontal median plane.

Table 4.3.1 Dipole magnet main parameters.

Number of Magnets	48
Bending Angle [degrees]	7.5
Bending Radius [m]	13.75
Inter Poles Gap [mm]	30
Magnetic Length [m]	1.8
Nominal magnetic Field [T]	0.723
Good Field Region ($\Delta B/B \leq 5\times10^{-3}$) [mm]	±20
Nominal Ampere-Turns	8718
Magnet Efficiency at Nominal Current	0.9882
Current [A]	1089
Number of Turns per Pole	8
Current Density [A/mm^2]	3.7
Yoke Weight [kg]	470
Coils Weight [kg]	153

Given the value of half gap h=15 mm and good field requirement $\Delta B/B \leq 5\times10^{-3}$, one can calculate the " pole overhang" [1,2] and thus pole size.

$$a_u = -h\left[0.36\ln\frac{\Delta B}{B} + 0.90\right] = -h\times\left[-1.08\right] = 16.2mm, \qquad (4.3.1)$$

for non-optimal shape and

$$a_o = -h\left[0.14\ln\frac{\Delta B}{B} + 0.25\right] = -h\times\left[-0.492\right] = 7.38mm, \qquad (4.3.2)$$

for optimized shape. Requiring ±20mm good field region along the beam orbit line, one finds the value of the pole width to be between 54.8 mm and 72.4 mm. The magnet yoke is curved to fit the beam orbit arc. The exact value of the width of the pole depends on optimization effectiveness. In our case, a pole width of 56 mm with shims mounted on the corners, reduces the gap at pole corners to 26 mm but provides the necessary good field region with some redundancy.

We chose a copper conductor of the size 12.6 ×14.0 mm^2 with a 6 mm diameter water-cooling hole. The cross section area of the conductor is 148 mm^2. For excitation of the 0.723 T field, 8718 Ampere-Turns are required (We calculated Ampere-Turns value by the formula $NI = Bh/\eta\mu_0$, where η = 0.988 is the magnet efficiency). In order to have a low number of turns for the conductor and subsequent low inductance, windings are joined in pairs in forming 8 turns. The nominal current is 1089 A that corresponds to 3.7 A/mm^2 of current density, which is quite acceptable value for coils with water- cooling.

The cross-sectional view of the magnet is shown in Figure 4.3.2.

The pole gap is 30 mm at the center provides room for the beam vacuum chamber. Simple shape shimming is used to provide a good field region with some redundancy.

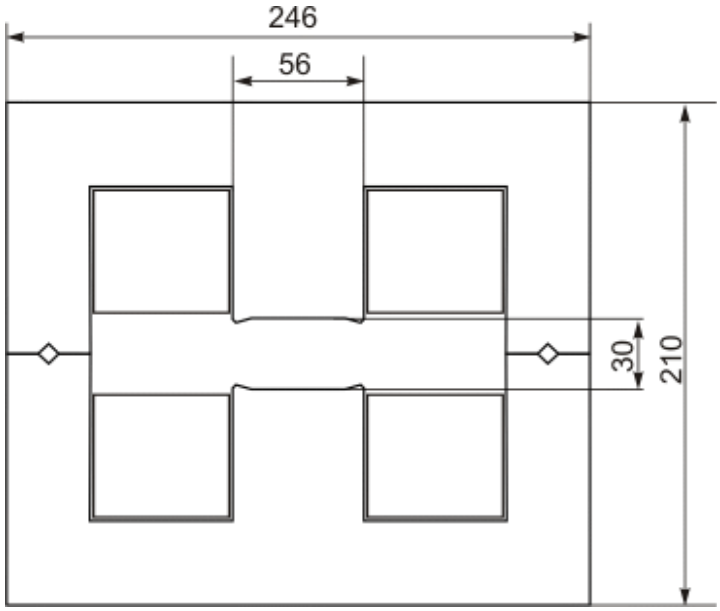

Figure 4.3.2 Booster dipole cross section.

The magnetic field is calculated using the POISSON code [3] and a field lines plot is shown in Figure 4.3.3. Only quarter of the magnet was considered in the simulation due to the 90 degree symmetry of the problem. The yoke sizes are adequate to avoid saturation and to provide high field quality (Magnet efficiency at 0.723 T field, which corresponds to a beam maximal energy of 3 GeV is 0.988).

The results of a harmonic analysis show the existence of a good quality field within the required good field region. Due to the magnet symmetry, quadrupole error fields are eliminated. The third and higher order terms in the field harmonic content at 14 mm normalization radius are at a level 0.1% of the dipole component or smaller. The results of field harmonic analysis are given in Fig. 4.3.4.

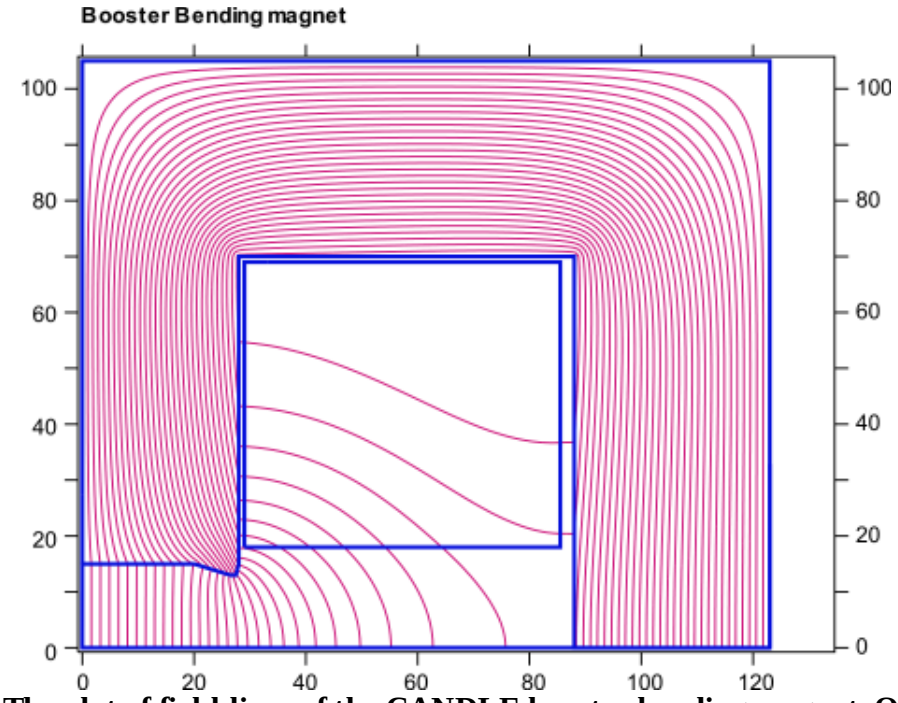

Fig. 4.3.3 The plot of field-lines of the CANDLE booster bending magnet. Only upper right quarter of the magnet cross-section is shown.

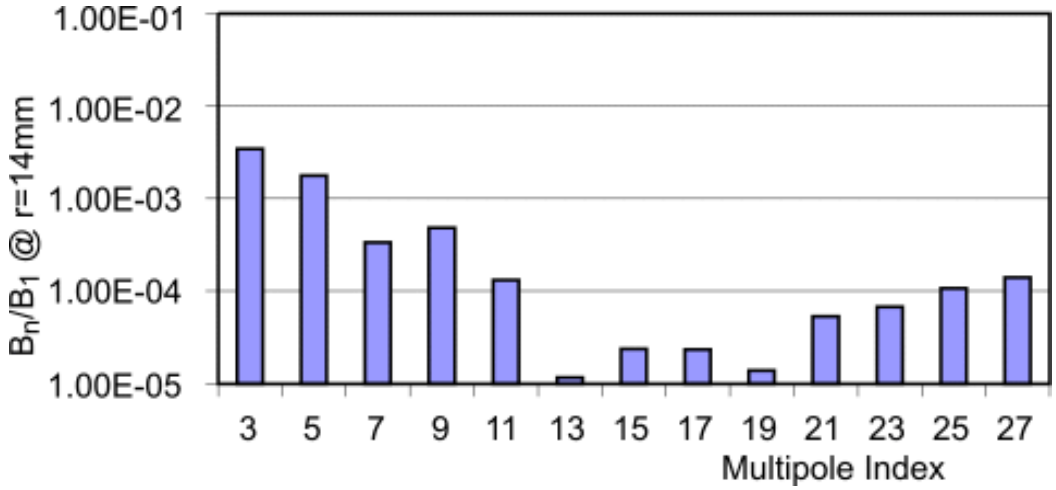

Fig. 4.3.4 Booster dipole magnet field random error multipole content. Normalization radius is equal to 14 mm. Errors are well bellow the required value of 5×10^{-3}.

Quadrupole magnets

The list of parameters of the booster quadrupole magnets is given in the Table 4.3.2. We have chosen a magnet design similar to that of SLS booster quadrupole magnet [4].

Table 4.3.2 Quadrupole magnet parameters

Number of magnets	64
Aperture radius [mm]	20
Magnetic length [m]	0.4
Gradient QF/QD [T/m]	13.3/-10.07
Ampere-turns	2865
Turns per pole	15
Current [A]	191
Current density [A/mm^2]	6
Conductor sizes [mm]	6.35mm×6.35mm with ∅3.15mm hole
Conductor cross section area [mm^2]	31.67
Lamination height [mm]	246
Lamination width [mm]	266
Conductor length per pole [m]	15
Magnet resistance [Ohm]	0.034
Magnet inductance [mH]	3.1

Coil turn number is low to make inductance low. We estimated magnet inductance to be about 3.1 mH. Three-dimensional simulation of the field of the such short magnets yet to be performed to take into account end fields accurately and calculate stored energy of the magnet in order to find more precise value of magnet inductance with the help of the formula $L = 2W / I^2$, where W is total stored energy and I is the excitation current. Accurate 3D analysis of the fringe fields is of great importance also for preventing the influence of the booster magnets stray fields on the storage ring beam during the injection time. The parameters of the quadrupole magnets are given in Table 4.3.2. The maximum of

the field flux density at pole tip $B_{\max} = B^{'} r = 0.36T$ is rather low to avoid significant stray fields ($B^{'} = 18T / m$ is the maximum design field gradient and $r = 20mm$ is the aperture radius).
Repetition rate is 2Hz and Eddy current losses in the coil and yoke as well as hysteresis losses in the yoke are negligible (Eddy current losses increase by square law and hysteresis losses increase linearly with A.C. frequency [5]). Magnet weight is about 155 kg.
The cross- sectional view of the booster quadrupole magnet is presented in figure 4.3.5.

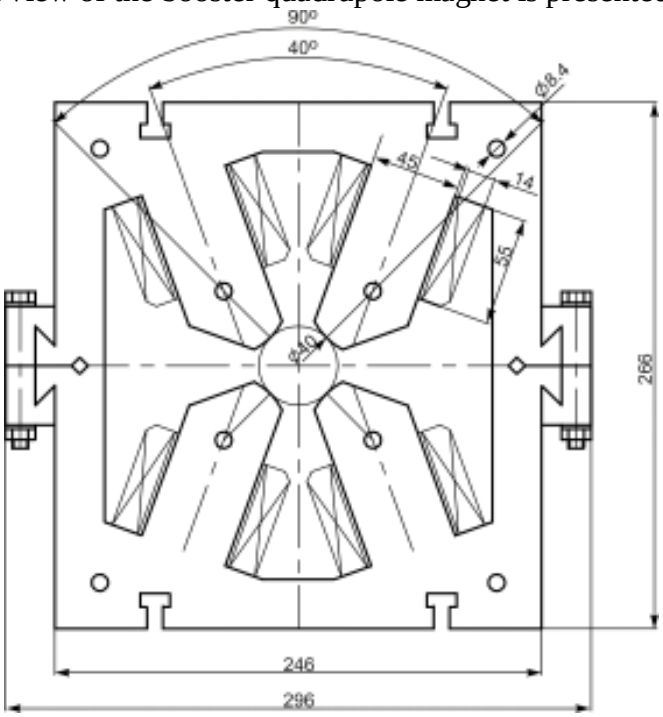

Figure 4.3.5 Booster quadrupole cross-section.

Sextupole Magnets
Principal parameters of the booster sextupole magnets are given in Table 4.3.3. Sextupole magnet design is based on the SLS booster sextupole magnet design [4]. It is intended to mount booster magnets on the inner wall of the storage ring and low weight of the sextupole is an asset. Chamfering of the magnet ends will be used to make magnet yoke length (0.15 m) equal to its magnetic length and therefore magnet weight will be less than 18.7 kg. Maximal field at pole tip will be

$$B_{\max} = 0.5B^{''} r^2 = 0.02T \,. \qquad (4.3.3)$$

Turns number should be kept as low as possible to have small inductance since booster magnets are being ramped with the repetition rate 2 Hz. Coils are made of copper conductor of 15 mm^2 cross section area and 16.5 m total length.
General experience shows that with current densities up to 2 A/mm^2 one can do without water-cooling and therefore avoid design complications and technical difficulties associated with it [1]. Having maximal current density equal to 1.8 A/mm^2 we consider natural convection cooling on the surface of the coil intensive enough to eliminate excessive heating of the magnet. The magnet parameters are given in Table 4.3.3. The cross-sectional view of the sextupole magnet is shown in Figure 4.3.6.

Table 4.3.3 Booster sextupole magnet parameters .

Number of magnets SF/SD	28 /28
Magnetic length [m]	0.15
Aperture radius [mm]	20
Sextupole strength SF/SD [T/m^2]	90.7/-114.6
Core weight [kg]	18.7
Coils weight [kg]	2.2
Ampere-turns	212
Turns per pole	8
Current [A]	27
Current Density [A/mm^2]	1.8
Conductor width [mm]	5
Conductor height [mm]	3
Conductor length per pole [m]	2.7
Conductor cross section area [mm^2]	15
Magnet width [m]	0.186
Magnet height [m]	0.170
Magnet resistance [Ohm]	0.02
Magnet inductance [mH]	1.4

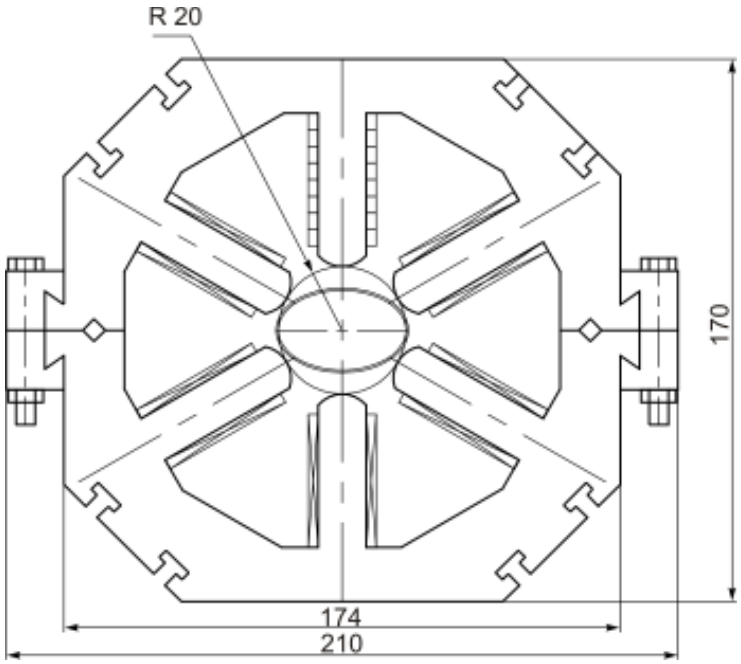

Figure 4.3.6 Booster sextupole magnet cross section.

Booster Injection Kicker Magnet

The main parameters of booster injection kicker magnet are given in the Table 4.3.4. Only one such magnet is used along with septum magnet to inject 100 MeV electron beam into booster. Its role is to bend injected beam by 10.5 mrad angle into booster orbit.

Table 4.3.4 Injector kicker magnet basic parameters.

Number of magnets	1
Magnet Length (m)	0.5
Deflection Angle (mrad)	10.5
Aperture (H×V, mm×mm)	40×25
Nominal Field (mT)	6.9
Peak Current (A)	212
Pulse Rising/Top/Fall Time (ns)	150/480/150
Repetition Rate (2Hz)	2
Inductance(μH)	≈1.3

We used windows frame design. Ferrite core window has sizes 35mm×70mm, and accommodates tick-wall ceramic beam chamber, which serves also as a support for the coils and ferrite core. One turn copper coil is used to produce required field 6.9 mT. Peak current is 210 Ampere. Magnet cross-sectional view with dimensions indicated is presented in the Figure 4.3.7.

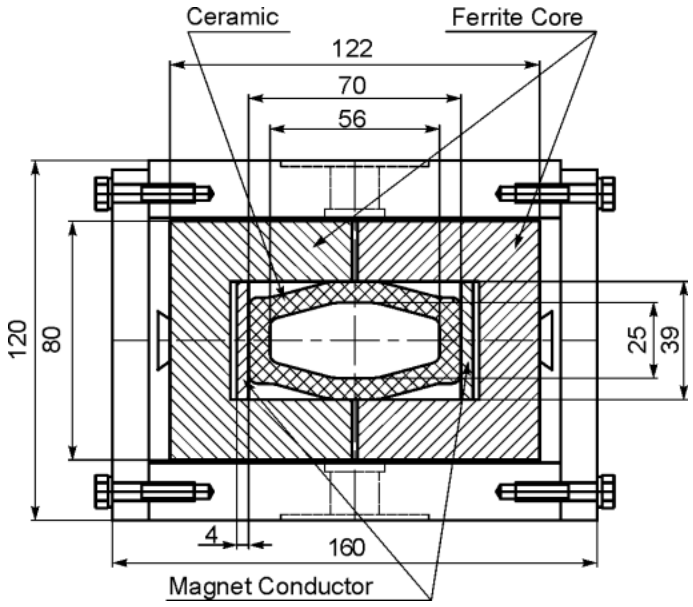

Fig. 4.3.7 Booster injection kicker cross section with ceramic beam chamber.

4.3.2 Vacuum System of the Booster

The booster ring has the geometry of a square with rounded corners. To optimize the division of the chamber into separate sectors, the ring is divided into 4 symmetrically located segments with a central angle equal to 90^o. Each segment is divided into 8 sectors, of which five are standard, two are main cells and one is straight. Each standard sector has a central angle of 15^o, main cell sectors of 12.5^o, and a straight sector is common for two neighboring segments. The compound parts of one segment are shown on figure 4.3.8.

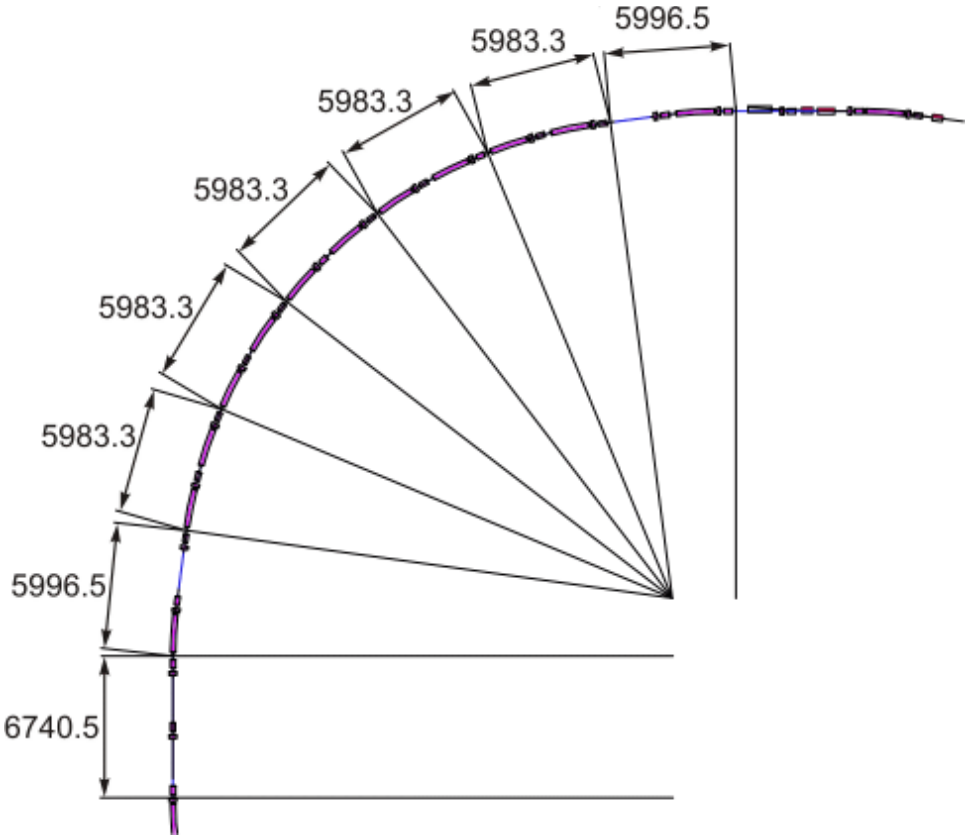

Fig.4.3.8 Booster ring segment

The length of the standard sector is 5983mm. The cross-section of the vacuum chamber is in the form of an ellipse, with inner vertical and horizontal sizes 25mm and 40mm, respectively. The vacuum chamber is made from the stainless steel. The elliptic profile of the chamber will be achieved by means of air-ejector technique with circular seamless thin-wall pipe, wall thickness equal to 0.7mm. A standard sector of the booster vacuum chamber is shown on figure 4.3.9.

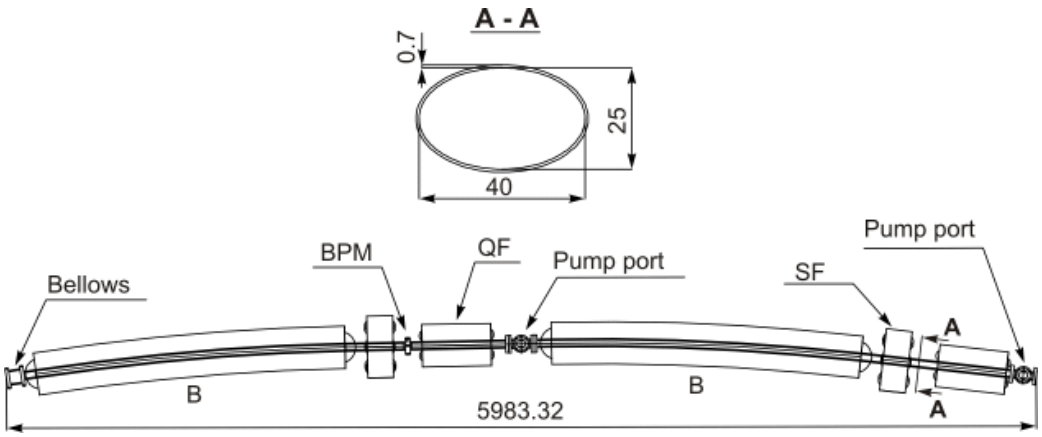

Fig. 4.3.9 Standard cell of the booster ring vacuum system.

As seen from the design, two pump ports are foreseen on the standard sector, one at the beginning of the sector and the second in the middle. The construction of the pump port is given in the figure 4.3.10.

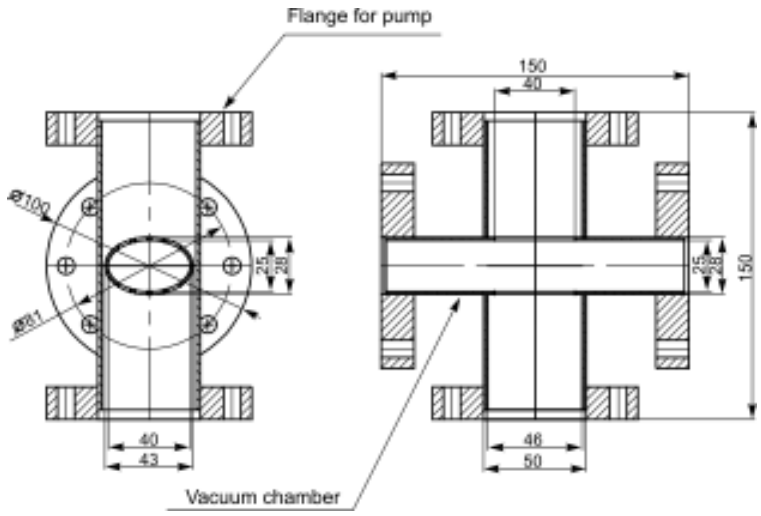

Fig. 4.3.10 Pump port of the booster vacuum system.

It is a crosspiece with 4 flanges, two of which – the lower and upper are used for spilling, with the other two longitudinal flanges being used to join the vacuum chambers. The thickness of the chamber wall inside the pump port is made thicker to increase the rigidity. Inside the pump ports, two longitudinal slots are milled on the chamber, through which the spilling is done. Thus, 4 pumps, two ionic and 2 turbo-molecular, are mounted on each standard sector. The nominal diameter of the spilling is 50mm. On the main cell as well as on the straight part, or the standard sector there are designated locations for mounting the BPMs. Construction of the node with a mounted BPM is given on figure 4.3.11a.

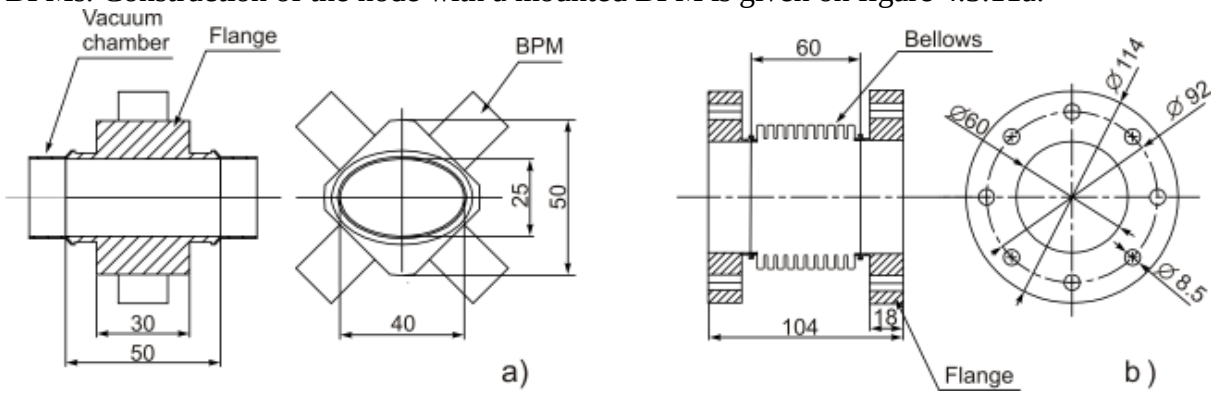

Fig. 4.3.11 Mounting of BPM (a) and bellow (b) on booster ring.

It is a flange with a 50mm diameter with 4 flat spots situated at 45^{o} to which the BPM blocks are welded. The flange has thin-walled nipples to which the vacuum chamber with flanged ends is welded. The sectors are joined to each other with bellows nodes. The construction of the bellows node is given in figure 4.3.11b. The conditional passage of the bellows is 60mm. The main cell and the straight parts are joined to each other similarly. The main cell and the straight part of the booster vacuum chamber are shown on figure 4.3.12. The length of the straight part is 6740.5mm, while the main cell length is 5996.2mm.

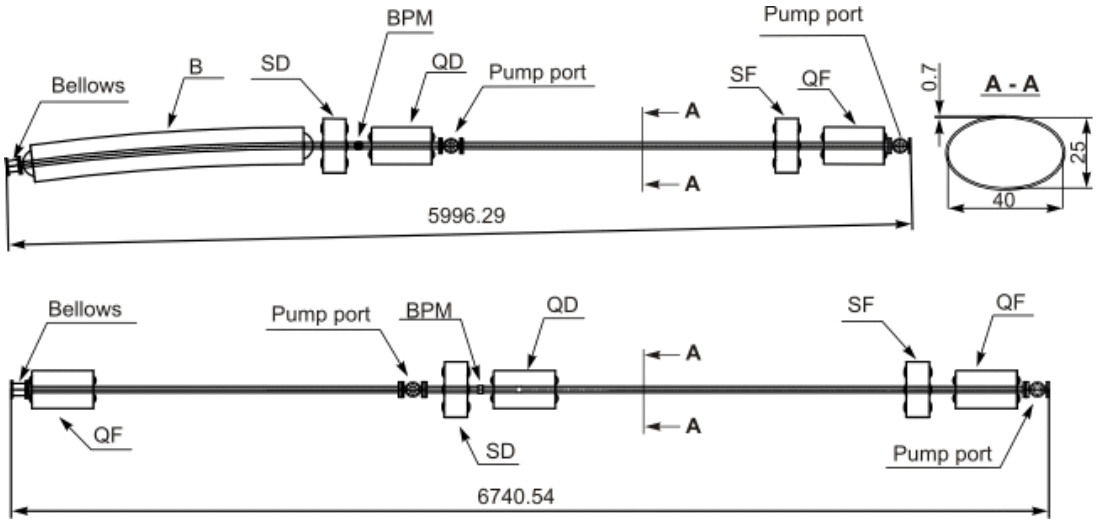

Fig. 4.3.12 Main cell and straight part of the booster vacuum chamber.

Specifications of the pumps with their quantity and capacity indications are given in table 4.3.5.

Table 4.3.5 The components of pumping system.

Pumps	**Quantity**	**Pumping rate/unit (liters/s)**	**Vacuum (Torr)**
Fore-vacuum pumps	22	5	10^{-2}
Ion-pumps	64	11	10^{-8}
Turbo-molecular pumps	16	50	10^{-7}

4.3.3 Power Supply System

The booster magnets power supply system has to provide a stable magnet ramping according to the beam energy increase from the injection energy of 100 MeV to final energy of 3 GeV.

The 100 MeV beam is injected into the booster with the dipole magnets field of 24.25 mT. At the maximum energy of 3 GeV, the magnetic field in dipoles reaches 0.7272 T.

Usually the Booster magnets power supply at the frequency of 10Hz is fulfilled by means of resonance “white circuit”. The resonance circuit is created by capacitor bank and inductance of the magnets windings, between which there is an exchange of electromagnetic energy. This circuit is proved at high repetition frequencies and has a good quality Q. With 2 Hz repetition frequency of the CANDLE booster synchrotron, the resonance “white circuit” scheme is useless. The “white circuit” scheme for 2 Hz booster will result in very small value of reactive energy cumulative in booster magnets (less than 30 kJ) which is evidently insufficient as the energy of the booster electromagnets per unit length should be larger than 3kJ/m (the circumference of the booster is 192m).

The magnetic structure of the booster lattice is of the separate function type, so the dipoles, quadrupole and sextupole families are powered by separate supplies in a strongly synchronized phase to keep the beam parameters in accordance with design specifications. The main stability requirements to the magnet power supply system, including ripples, are

- Dipole magnets -0.01%
- Quadrupole magnets –0.1 %
- Sextupole magnets -0.5%

AC power for the booster magnet supply system is provided by separate transformer group. DC voltage and current waveforms are computer controlled to provide the optimal beam ramping process, as well as the clean filling of the appropriate RF buckets of the storage ring. The booster repetition rate is 2 Hz so the 220 ms is allowed for the magnet DC current ramp from 0 to nominal value that corresponds to 3 GeV beam energy. The power supply is designed with overhead of 10 % to maintain the acceleration of 3.3 GeV electron beam if desired. The main parameters of the booster magnet power supplies are summarized in Table 4.3.6.

Table 4.3.6 Main parameters of the magnet power supply.

Magnets		**Quantity**	**Family total**		
			I (A)	V,dc (V)	R (Ω)
Bending		48 (in series)	1089	394	0.365
Quadrupole family QF		32 (in series)	191	206.3	1.08
Quadrupole family QD		32 (in series)	191	206.3	1.08
Sextupole family SF		28 (in series)	27	16	0.56
Sextupole family SD		28 (in series)	27	16	0.56
Correction dipoles	Horizontal	16	22	14	0.696
	Vertical	16	9.8	6	1.381

Bending Magnet Power Supplies

The booster synchrotron contains 48 identical dipole magnets. These magnets are electrically connected in series and require a single SCR (Silicon Controlled Rectifier) power supply that is capable for operation in both the rectification mode and the inversion mode. The operating repetition rate of the synchrotron is 2 Hz, and 220 ms is allowed for the magnet current to increase from 0 to 1089 A.

As soon as beam extraction is accomplished, the SCRs of the power supply are phased to inversion, and the energy stored in the magnets returns to the AC power line as the magnet current decreases.

The voltage swing is limited to less than 1000 V. This is achieved by using two power supply units with grounded midpoint. The rectifier is divided into two parts. Each part is presented as a 12-phase rectifier, which provides minimal pulsations of the problem voltage [9].

The scheme consists of two series DC-choppers. Such cascade connection allows transfer the direct current of power through that line. The accumulating capacity is feeding two parallel- connected 2Q choppers. In series connected windings of the 48 booster dipole magnets have the resistance of 0.36Ω and the inductance of 43mH**.** The calculated summed current in the circuit is equal to 1089A, when the maximal frequency is 2Hz. It is necessary to provide 600V peak voltage of the power supply for the given peak current. It results in a total complement of four power units. Each power unit carries the half of the current, i.e. 550A and half the voltage, i.e. 250V.

On the assumption of the above mentioned, a switched mode power supply is used for the booster magnets. The principal block-scheme of the booster dipoles power supply is similar to that of developed for ALS and SLS boosters and is given in Fig. 4.3.13. The given scheme allows the usage of sinusoidal current frequencies up to several Hz. The Insulated Gate Bipolar Transistors are foreseen as key elements in the chopping circuits.

These transistors allow switching frequency 10kHz, which is necessary for the functioning of the device. When the synchrotron booster functions with the impulse frequency of 2Hz, the power supply varies from 520kW to -140kW (minimal value). The average power for the dipole magnets is 150kW.

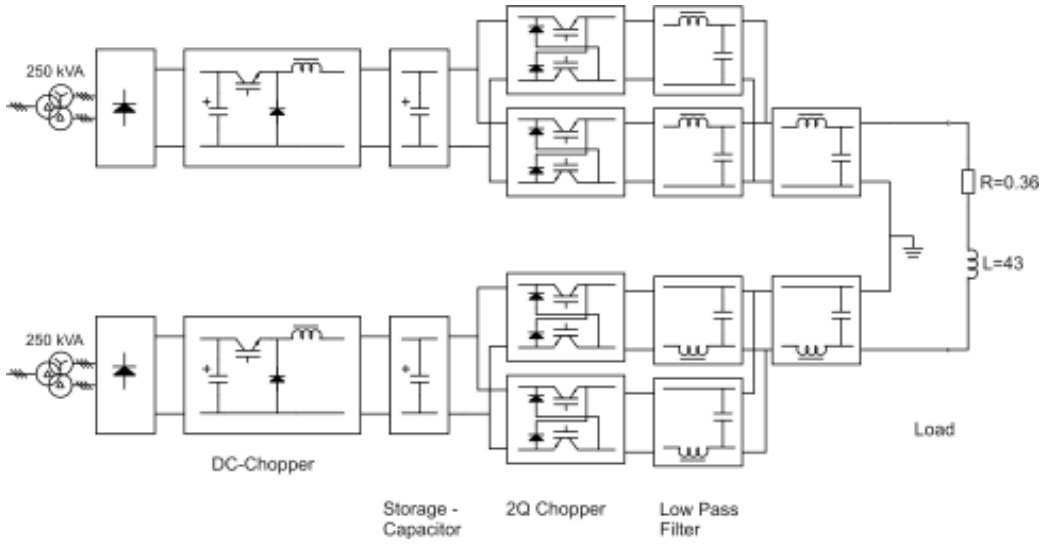

Fig. 4.3.13 Principal block-scheme of the booster dipole magnet power supply

Quadrupole Magnet Power Supplies

The 64 quadrupole magnets in booster synchrotron are divided into two families; focusing (QF) and defocusing (QD) magnets. Each family has 32 magnets powered by two separate power supply systems consisting of two DC power supplies that connected in series. The principal scheme is shown in Fig. 4.3.14.

One power supply is of SCR type, which can operate in the rectification mode or in the inversion mode. This power supply provides the voltage required to obtain the desired current waveform.The second supply is of another SCR type whose output voltage can be controlled from 0 to 150 V. This power supply also has a series transistor regulator to regulate the output current of both supplies. The transistor regulator is required to obtain the closed-loop frequency response necessary to synchronize the quadrupole and dipole current ramping within 0.1% [10].

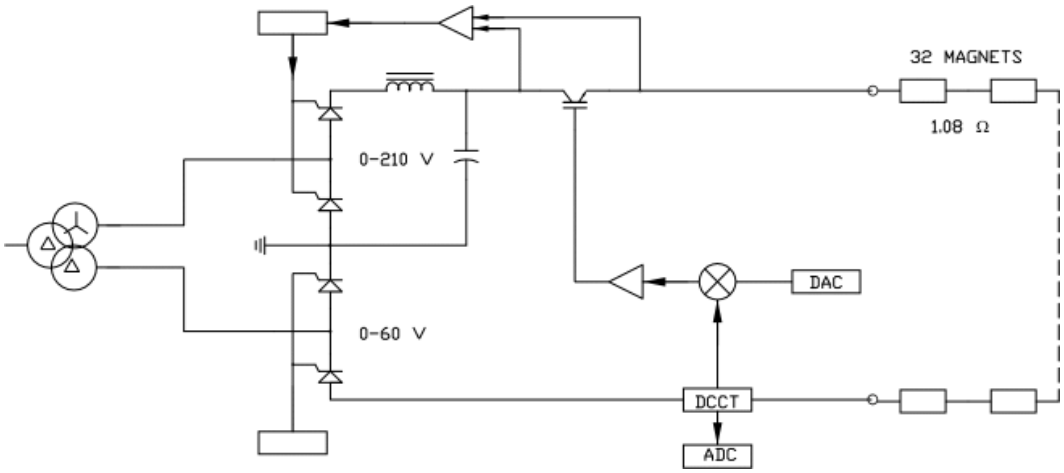

Fig. 4.3.14 The principal scheme of the quadrupole magnet power supply.

Sextupole Magnet Power Supplies

The 56 sextupole magnets of the booster synchrotron are divided into two families (SF and SD): each family consists of 28 magnets connected in series. Each of the magnets is rated 0.54V, 27A. A transistor regulated power supply (rated 16V, 27A) is used for each family. Analog reference voltages, applied to their regulation circuits, control the outputs of these supplies**.** Magnet currents are monitored by ADC connected to a local computer; the computer controls a DAC that furnishes the analog reference voltage necessary to achieve the desired tracking accuracy.

Correction Magnet Power Supplies

There are 32 correction coils in booster synchrotron, 16 for vertical correction and 16 for horizontal correction.

Each of the 32 correction coils is powered by a separate, commercially available bipolar power supply. Each horizontal correction coil requires 400 VA (14V, 22A) and each vertical correction coil requires 100 VA (6V, 9.8A) power supply capacity.

References

1. J. Tanabe "Lectures" January, 2000.
2. K. Halbach "Special Topics in Magnetics" in Handbook of Accelerator Physics and Engineering, Singapore, 1999.
3. Programs available from LANL Accelerator Code Group, LA-UP-90-1766,1990.
4. SLS Design Report
5. N. Marks "Conventional Magnets" in Proc. of CERN CAS, 1994-01 v2, 1994.
6. L. Schulz, Stainless Steel Vacuum Chambers, 25th ICFA Advanced Beam Dynamics Workshop: SSILS, 2001.
7. G.L. Saksaganskii, Getter and Getter-ion Vacuum Pumps, Harwood Academic Publications, Switzerland, 1994.
8. G. Irminger, M. Horvat, F. Jenni "A 3 Hz, 1MW peak Bending Magnet Power Supply for the SLS", 5 November, 1998.
9. 1-2 GeV SRS Conceptual Design Report, Lawrence Berkeley Laboratory University of California, July 1986